Materials Sciences and Applications, 2012, 3, 733-738
http://dx.doi.org/10.4236/msa.2012.310107 Published Online October 2012 (http://www.SciRP.org/journal/msa)

Direct Decomposition of NO into N_2 and O_2 over C-Type Cubic Y_2O_3-Tb_4O_7-ZrO_2

Toshiyuki Masui, Shunji Uejima, Soichiro Tsujimoto, Nobuhito Imanaka*

Department of Applied Chemistry, Faculty of Engineering, Osaka University, Suita, Japan.
Email: *imanaka@chem.eng.osaka-u.ac.jp

Received July 14th, 2012; revised August 15th, 2012; accepted September 16th, 2012

ABSTRACT

Catalytic activities for direct NO decomposition were investigated over C-type cubic Y_2O_3-Tb_4O_7-ZrO_2 prepared by a co-precipitation method. The NO decomposition activity was enhanced by partial substitution of the yttrium sites with terbium in a $(Y_{0.97}Zr_{0.03})_2O_{3.03}$ catalyst, which shows high NO decomposition activity. Among the catalysts synthesized in this study, the $(Y_{0.67}Tb_{0.30}Zr_{0.03})_2O_{3.33}$ catalyst exhibited the highest NO decomposition activity; NO conversion to N_2 was as high as 67% at 900˚C in the absence of O_2 (NO/He atmosphere), and a relatively high conversion ratio was observed even in the presence of O_2 or CO_2, compared with those obtained over conventional direct NO decomposition catalysts. These results indicate that the C-type cubic Y_2O_3-Tb_4O_7-ZrO_2 catalyst is a new potential candidate for direct NO decomposition.

Keywords: Nitrogen Monoxide; Direct Decomposition; Catalyst; Rare Earth Oxide; C-Type Cubic Structure

1. Introduction

Nitrogen oxides (NO_x) are not only harmful to human beings, but are also responsible for photochemical smog and acid rain when present in relatively high levels in the atmosphere. NO_x is mainly produced by the high-temperature combustion of fossil fuels such as petroleum in the engines of vehicles and ships, or coke in large-size boilers of factories. NO_x species in exhaust gases emitted at high temperatures are composed principally of thermodynamically stable NO and a negligible amount of NO_2. Therefore, studies on the catalytic decomposition of NO_x should focus on NO.

Several NO reduction processes have been proposed for NO_x removal. Among them, selective catalytic reduction (SCR) methods employing ammonia or urea have been extensively studied and applied in diesel engines and large-size boilers [1]. The SCR methods have sufficient NO decomposition efficiency and a stable reaction process at high temperatures. However, separate specialized equipment is necessary to supply the reducing agents. Moreover, it is absolutely essential to ensure secure control systems due to the high toxicity and flammability of ammonia.

In contrast to the above processes employing ammonia or urea, direct catalytic decomposition of NO into N_2 and O_2 ($2NO \rightarrow N_2 + O_2$) is the most ideal route for NO_x removal, because no reducing agents and no special equipment are required. A number of materials, such as zeolites [2,3], perovskites [4-6], and other complex oxides [7-18], have been proposed as active catalysts for direct NO decomposition. However, the NO decomposition activity of these conventional catalysts is significantly decreased in the presence of O_2 and CO_2, due to strong adsorption of these molecules on the surface of the catalysts. Oxygen molecules produced by NO decomposition as well as those present in the gas phase adsorb on the catalyst surface and interfere with the catalytic reaction. In addition, a number of active direct NO decomposition catalysts contain highly basic alkaline and alkaline earth ions in the lattice. Among them, catalysts containing Ba typically exhibit high NO decomposition activities, because NO is acidic and adsorption of NO on the surface of the catalyst is significantly enhanced with increasing basicity of the catalyst. However, the high basicity also facilitates adsorption of CO_2. As a result, catalyst poisoning by CO_2 adsorption becomes a serious problem.

To realize high activities for direct NO decomposition, it is important to design a novel catalyst that is not influenced by the presence of CO_2 or O_2. Accordingly, we focused on C-type cubic rare earth oxides. Rare earth oxides can form three types of crystal structures, A-(hexagonal), B-(monoclinic), and C-types (cubic), depending on the ionic size of the respective rare earth element [19]. Among these, the C-type cubic structure

*Corresponding author.

has the largest interstitial open space. It has been generally accepted that large open spaces in a catalyst play an important role in direct NO decomposition, and for this reason the C-type cubic rare earth oxide is suitable as a direct NO removal catalyst. Furthermore, in our previous works, we found that several C-type cubic rare earth oxide catalysts can exhibit high activities for direct NO decomposition even in the presence of O_2 [20-25] and that exclusion of alkaline earth ions from the catalyst lattice is significantly effective to induce CO_2 tolerance [25,26].

In the present study, $(Y_{0.97-x}Tb_xZr_{0.03})_2O_{3.03+\delta}$ solid solutions (x = 0, 0.10, 0.20, 0.30, and 0.40), which adopt a C-type cubic structure, were designed as novel NO decomposition catalysts. In these catalysts, a fraction of the yttrium sites in $(Y_{0.97}Zr_{0.03})_2O_{3.03}$, which showed the highest NO decomposition activity in $(Y_{1-y}Zr_y)_2O_{3+y}$ ($0 \le y \le 0.10$) [24], was substituted with terbium to inhibit catalyst poisoning by O_2 and CO_2, utilizing the redox property of $Tb^{4+/3+}$ [23,25] for effective direct NO decomposition.

2. Experimental

2.1. Catalyst Preparation

The C-type cubic $(Y_{0.97-x}Tb_xZr_{0.03})_2O_{3.03+\delta}$ (x = 0, 0.10, 0.20, 0.30, and 0.40) catalysts were synthesized by a co-precipitation method, where the zirconium content was fixed at 3 mol% for the reason mentioned above. A stoichiometric mixture of 1 mol·dm^{-3} $Y(NO_3)_3$, 0.1 mol·dm^{-3} $Tb(NO_3)_3$, and 0.1 mol·dm^{-3} $ZrO(NO_3)_2$ aqueous solutions was added to a 1.0 mol·dm^{-3} ammonium carbonate solution with stirring. The pH of the mixture was adjusted to 10 by dropwise addition of 9% ammonia solution. After stirring at room temperature for 6 h, the resulting precipitate was collected by filtration, washed several times with deionized water, and then dried at 80˚C for 6 h. The powder was then ground in an agate mortar and finally calcined at 900˚C in air for 6 h.

2.2. Characterization

The catalysts were characterized by X-ray powder diffraction (XRD; Rigaku SmartLab) with CuKα radiation. XRD patterns were recorded in the 2α range from 10˚ to 70˚. The sample compositions were analyzed by X-ray fluorescence spectrometry (XRF; Rigaku, ZSX100e) and the specific surface area was measured by the Brunauer-Emmett-Teller (BET) method using nitrogen adsorption at −196˚C with a Micromeritics TriStar 3000 adsorption analyzer.

2.3. Catalyst Test

The NO decomposition reaction was carried out in a conventional fixed-bed flow reactor with a 10-mm-diameter quartz glass tube. A gas mixture of 1 vol% NO and He (balance) was fed at a rate of 10 cm^3·min^{-1} over 0.5 g of catalyst. The W/F ratio, where W and F are the catalyst weight and gas flow rate, respectively, was adjusted to 3.0 g·s·cm^{-3}. The gas composition was analyzed using a gas chromatograph (Shimadzu GC-8A) with a thermal conductivity detector (TCD), a molecular sieve 5 A column for NO, N_2, and O_2, and a Polapak-Q column for N_2O separation. The activity of each catalyst was evaluated in terms of NO conversion to N_2.

The effect of the presence of O_2 or CO_2 was measured by mixing each gas species with the reactant gas. The concentrations of the additional gases and NO were controlled by changing the feed rate of He as the balance gas to maintain a total reactant flow rate of 10 cm^3·min^{-1}.

2.4. Temperature Programmed Desorption

Temperature-programmed desorption (TPD) measurements of O_2 was carried out after adsorption of O_2 at 600˚C for 1 h. After heating the catalyst in a flow of He (30 cm^3·min^{-1}) at 600˚C for 30 min, the catalyst was exposed to O_2 (1 atm) at the same temperature for 1 h, and then cooled to 50˚C. After evacuation at 50˚C for 30 min, the catalyst was heated under a flow of He at a heating rate of 10˚C·min^{-1} and the desorbed gas was monitored using a gas chromatograph with a catalysis analyzer (BELCAT-B BEL JAPAN). In the case of CO_2-TPD, the catalyst was heated in a flow of He (30 cm^3·min^{-1}) at 600˚C for 1 h, and subsequently in a flow of H_2 (30 cm^3·min^{-1}) at 600˚C for 30 min. The catalyst was cooled in a flow of He to 50˚C, and was then exposed to CO_2 (1 atm) at this temperature for 1 h. After evacuation at 50˚C for 30 min, the catalyst was heated under a flow of He at a heating rate of 10˚C·min^{-1}.

3. Results and Discussion

3.1. Characterization of the Catalysts

Figure 1 shows XRD patterns of the $(Y_{0.97-x}Tb_xZr_{0.03})_2O_{3.03+\delta}$ catalysts (x = 0, 0.10, 0.20, 0.30, and 0.40). C-type cubic rare earth oxide with a single phase structure (PDF-ICDD 41-1105 for Y_2O_3) was successfully obtained for all samples and no crystalline impurities were observed. The catalyst compositions, as determined using XRF, the lattice constants, and the BET surface area of the $(Y_{0.97-x}Tb_xZr_{0.03})_2O_{3.03+\delta}$ catalysts are summarized in **Table 1**. The cubic lattice parameter of $(Y_{0.97-x}Tb_xZr_{0.03})_2O_{3.03+\delta}$ gradually decreased with the x value, because ionic sizes of Y^{3+} and Tb^{4+} with a six-fold coordination are 0.1040 nm [27] and 0.0900 nm [27], respectively. When the smaller Tb^{4+} occupies the lattice position of Y^{3+} in $(Y_{0.97}Zr_{0.03})_2O_{3.03}$, the lattice parameter

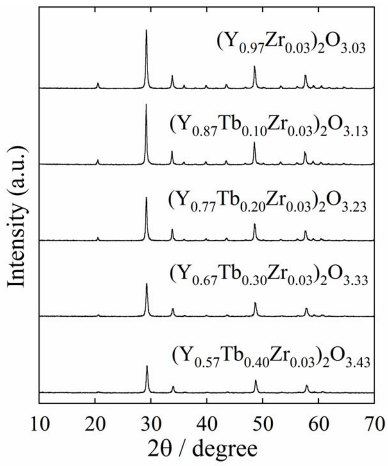

Figure 1. XRD patterns of the $(Y_{0.97-x}Tb_xZr_{0.03})_2O_{3.03+\delta}$ catalysts (x = 0, 0.10, 0.20, 0.30, and 0.40).

Table 1. Composition, lattice constant, and BET surface area of the $(Y_{0.97-x}Tb_xZr_{0.03})_2O_{3.03+\delta}$ catalysts.

Composition	Lattice constant	BET surface area
	/nm	$/m^2 \cdot g^{-1}$
$(Y_{0.97}Zr_{0.03})_2O_{3.03}$	1.0609	20.6
$(Y_{0.87}Tb_{0.10}Zr_{0.03})_2O_{3.13}$	1.0600	15.6
$(Y_{0.77}Tb_{0.20}Zr_{0.03})_2O_{3.23}$	1.0588	16.0
$(Y_{0.67}Tb_{0.30}Zr_{0.03})_2O_{3.33}$	1.0573	22.0
$(Y_{0.57}Tb_{0.40}Zr_{0.03})_2O_{3.43}$	1.0561	21.5

decreases monotonically with increasing Tb^{4+} content. The results indicate that C-type cubic solid solutions were successfully formed for all samples. The BET specific surface area was slightly affected by the introduction of Tb^{4+} into the $(Y_{0.97}Zr_{0.03})_2O_{3.03}$ lattice.

3.2. NO Decomposition Activity

Figure 2 depicts the temperature dependencies of the N_2 yield for the $(Y_{0.97-x}Tb_xZr_{0.03})_2O_{3.03+\delta}$ catalysts (x = 0, 0.10, 0.20, 0.30, and 0.40). Initial NO decomposition activity appeared at 550˚C and the N_2 yield increased monotonically with reaction temperature. The formation of N_2O was not detected between 400 and 900˚C. **Figure 3** shows the dependence of NO conversion into N_2 at 900˚C on the composition of the C-type cubic $(Y_{0.97-x}Tb_xZr_{0.03})_2O_{3.03+\delta}$ catalysts. The catalytic activity increased with the x value, and the highest catalytic activity was obtained for the $(Y_{0.67}Tb_{0.30}Zr_{0.03})_2O_{3.33}$ composition, where the N_2 yield obtained over this catalyst was 67%.

3.3. Effect of the Presence of O_2 or CO_2

The effect of the presence of O_2 or CO_2 on the N_2 yield

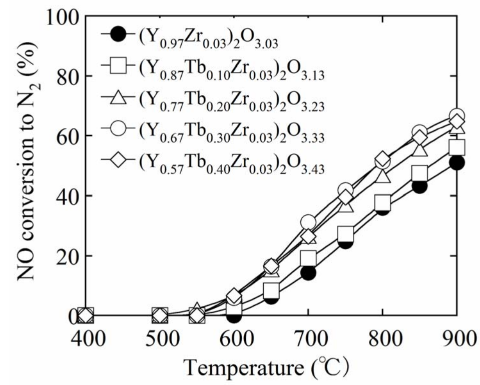

Figure 2. Temperature dependence of the N_2 yield obtained over the $(Y_{0.97-x}Tb_xZr_{0.03})_2O_{3.03+\delta}$ catalysts (x = 0, 0.10, 0.20, 0.30, and 0.40) (NO: 1 vol%, He; balance, W/F = 3.0 $g \cdot s \cdot cm^{-3}$).

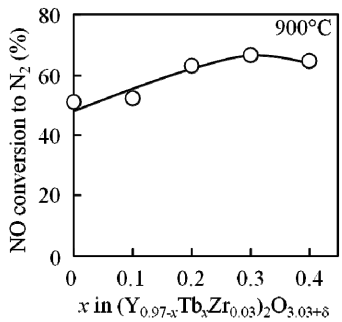

Figure 3. Dependence of NO conversion into N_2 at 900˚C on the terbium concentration in the $(Y_{0.97-x}Tb_xZr_{0.03})_2O_{3.03+\delta}$ catalysts (NO: 1 vol%, He; balance, W/F = 3.0 $g \cdot s \cdot cm^{-3}$).

obtained over the $(Y_{0.67}Tb_{0.30}Zr_{0.03})_2O_{3.33}$ catalyst at 900˚C was also examined, and the results are presented in **Figure 4**. In the presence of O_2, the N_2 yield for $(Y_{0.67}Tb_{0.30}Zr_{0.03})_2O_{3.33}$ decreased from 67 to 53% until the content reached 1 vol%, but became almost constant in the range from 1 to 5 vol%. As a result, NO decomposition activity as high as 47% was maintained, even in the presence of 5 vol% O_2, and the activity did not deteriorate during the 10-h catalytic test. This conversion ratio in the presence of 5 vol% O_2 (47%) was higher than that for C-type cubic $(Yb_{0.50}Tb_{0.50})_2O_{3\pm\delta}$ (35%) [25].

In contrast, the effect of CO_2 on the NO decomposition activity was relatively larger than that for O_2, but the decreasing tendency of the N_2 yield with the increase in the partial pressure of CO_2 was similar to that observed for O_2. Since CO_2 is acidic, adsorption of CO_2 on the basic sites of the catalyst surface will inhibit NO adsorption on the open space sites of the catalyst. However, for the $(Y_{0.67}Tb_{0.30}Zr_{0.03})_2O_{3.33}$ catalyst, a high N_2 yield of 36% was maintained even in the presence of 5 vol% CO_2, which is higher than those for the $(Yb_{0.50}Tb_{0.50})_2O_{3\pm\delta}$ (34%) [25], $Ba_{0.8}La_{0.2}Mn_{0.8}Mg_{0.2}O_3$ (20% at 850˚C) [12], and $La_{0.8}Sr_{0.2}CoO_3$ (10% at 800˚C) catalysts [15].

Furthermore, the catalytic activity was recovered when the catalytic test was carried out again in the absence of CO_2 (1 vol% NO/He), which indicates that the decrease in NO decomposition activity is caused by the adsorption of CO_2 on the catalyst. In addition, the XRD patterns of the $(Y_{0.67}Tb_{0.30}Zr_{0.03})_2O_{3.33}$ catalyst were the same before and after the reactions.

3.4. O_2 and CO_2 Desorption Profiles

As mentioned above, the present $(Y_{0.67}Tb_{0.30}Zr_{0.03})_2O_{3.33}$ catalyst showed relatively high catalytic activity even in the presence of O_2 or CO_2. To facilitate direct NO decomposition, it is important that these coexisting gases desorb from the surface of the catalyst easily. Therefore, desorption behavior of O_2 and CO_2 adsorbed on $(Y_{0.67}Tb_{0.30}Zr_{0.03})_2O_{3.33}$ was characterized by TPD measurements.

Figure 5 shows O_2 and CO_2 desorption profiles (O_2-TPD and CO_2-TPD) for $(Y_{0.67}Tb_{0.30}Zr_{0.03})_2O_{3.33}$. In references [5,6,12], catalysts that demonstrated low-temperature O_2 desorption exhibited high activities for NO decomposition. In the present case, a single O_2 desorption peak was observed at 470˚C for the $(Y_{0.67}Tb_{0.30}Zr_{0.03})_2O_{3.33}$ catalyst, whereas that for $(Yb_{0.50}Tb_{0.50})_2O_{3\pm\delta}$ was 510˚C. In general, catalysts with weak oxygen adsorption exhibit higher NO decomposition activities. Therefore, the $(Y_{0.67}Tb_{0.30}Zr_{0.03})_2O_{3.33}$ catalyst showed high NO decomposition activity even in the presence of O_2.

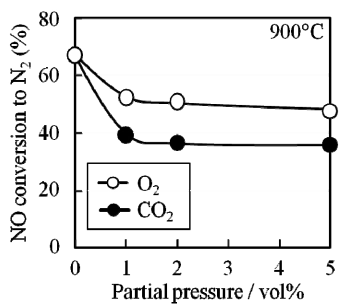

Figure 4. Effect of the presence of O_2 or CO_2 on the N_2 yield obtained over the $(Y_{0.67}Tb_{0.30}Zr_{0.03})_2O_{3.33}$ catalyst at 900˚C (NO: 1 vol%, O_2: 0 - 5 vol%, CO_2: 0 - 5 vol%, He; balance, W/F = 3.0 g·s·cm^{-3}).

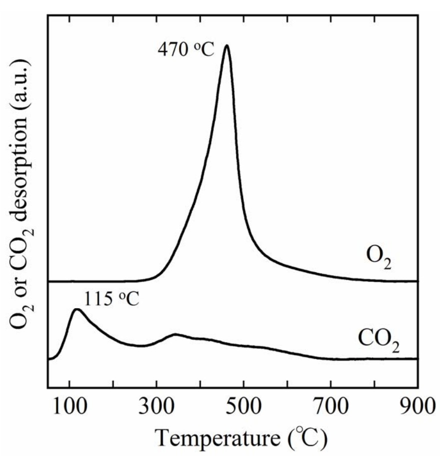

Figure 5. O_2 and CO_2 desorption profiles (O_2-TPD and CO_2-TPD) for $(Y_{0.67}Tb_{0.30}Zr_{0.03})_2O_{3.33}$.

In the case of CO_2, the CO_2 desorption peak was observed at 115˚C, which is much lower than those seen for $Ba_{0.8}La_{0.2}Mn_{0.8}Mg_{0.2}O_3$ (700˚C) [14] and $La_{0.8}Sr_{0.2}CoO_3$ (750˚C) [15]. The adsorption strength of CO_2 correlates with the desorption temperature observed in TPD, and the lower the CO_2 desorption temperature is, the weaker the adsorption strength becomes. Although the weakly adsorbed CO_2 may block the active site for NO decomposition in the $(Y_{0.67}Tb_{0.30}Zr_{0.03})_2O_{3.33}$ catalyst, the adsorption strength of CO_2 on this catalyst is quite weak. As a result, the NO decomposition activity was not significantly suppressed by the CO_2 coexistence. This consideration is supported by the result mentioned above that the N_2 yield obtained at 900˚C in the presence of 5 vol% CO_2 over the present $(Y_{0.67}Tb_{0.30}Zr_{0.03})_2O_{3.33}$ catalyst (36%) was almost equivalent to that over $(Yb_{0.50}Tb_{0.50})_2O_{3\pm\delta}$ (34%), because the CO_2 desorption peak was observed at 115˚C and 125˚C for the former ant the latter, respectively.

4. Conclusion

C-type cubic $(Y_{0.97-x}Tb_xZr_{0.03})_2O_{3.03+\delta}$ (x = 0, 0.10, 0.20, 0.30, and 0.40) catalysts, in which the yttrium site was partially substituted with terbium, were found to exhibit high catalytic activity for direct NO decomposition. The highest catalytic activity was obtained for $(Y_{0.67}Tb_{0.30}Zr_{0.03})_2O_{3.33}$. It is noteworthy that the catalytic activity was maintained at a high conversion ratio even in the presence of O_2 or CO_2. Therefore, the $(Y_{0.67}Tb_{0.30}Zr_{0.03})_2O_{3.33}$ catalyst is expected to be a new potential candidate as a direct NO decomposition catalyst.

5. Acknowledgements

This research was supported by the Industrial Technology Research Grant Program ’08 (Project ID: 08B42001a) from the New Energy and Industrial Technology Development Organization (NEDO) of Japan, and by the Steel Industry Foundation for the Advancement of Environmental Protection Technology (SEPT).

REFERENCES

[1] Z. Liu and S. I. Woo, “Recent Advances in Catalytic DeNO$_x$ Science and Technology,” *Catalysis Reviews*: *Science and Engineering*, Vol. 48, No. 1, 2006, pp. 43-89. doi:10.1080/01614940500439891

[2] M. Iwamoto, H. Yahiro, K. Tanda, N. Mizuno, Y. Mine

and S. Kagawa, "Removal of Nitrogen Monoxide through a Novel Catalytic Process. 1. Decomposition on Excessively Copper Ion Exchanged ZSM-5 Zeolites," *The Journal of Physical Chemistry*, Vol. 95, No. 9, 1991, pp. 3727-3730. doi:10.1021/j100162a053

[3] B. L. Trout, A. K. Chakraborty and A. T. Bell, "Analysis of the Thermochemistry of NO_x Decomposition over CuZSM-5 Based on Quantum Chemical and Statistical Mechanical Calculations," *The Journal of Physical Chemistry*, Vol. 100, No. 44, 1996, pp. 17582-17592. doi:10.1021/jp961470b

[4] Y. Teraoka, T. Harada and S. Kagawa, "Reaction Mechanism of Direct Decomposition of Nitric Oxide over Co- and Mn-Based Perovskite-Type Oxides," *Journal of the Chemical Society*, *Faraday Transactions*, Vol. 94, No. 13, 1998, pp. 1887-1891. doi:10.1039/a800872h

[5] T. Ishihara, M. Ando, K. Sada, K. Takiishi, K. Yamada, H. Nishiguchi and Y. Takita, "Direct Decomposition of NO into N_2 and O_2 over La(Ba)Mn(In)O_3 Perovskite Oxide," *Journal of Catalysis*, Vol. 220, No. 1, 2003, pp. 104-114. doi:10.1016/S0021-9517(03)00265-3

[6] H. Iwakuni, Y. Shinmyou, H. Yano, H. Matsumoto and T. Ishihara, "Direct Decomposition of NO into N_2 and O_2 on $BaMnO_3$-Based Perovskite Oxides," *Applied Catalysis B*: *Environmental*, Vol. 74, No. 3-4, 2007, pp. 299-306. doi:10.1016/j.apcatb.2007.02.020

[7] M. Haneda, Y. Kintaichi, N. Bion and H. Hamada, "Alkali Metal-Doped Cobalt Oxide Catalysts for NO Decomposition," *Applied Catalysis B*: *Environmental*, Vol. 46, No. 3, 2003, pp. 473-482. doi:10.1016/S0926-3373(03)00287-X

[8] S. Xie, G. Mestl, M. P. Rosynek and J. H. Lunsford, "Decomposition of Nitric Oxide over Barium Oxide Supported on Magnesium Oxide. 1. Catalytic Results and *in Situ* Raman Spectroscopic Evidence for a Barium-Nitro Intermediate," *Journal of the American Chemical Society*, Vol. 119, No. 42, 1997, pp. 10186-10191. doi:10.1021/ja970809k

[9] Z. Liu, J. Hao, L. Fu and T. Zhu, "Study of Ag/$La_{0.6}Ce_{0.4}CoO_3$ Catalysts for Direct Decomposition and Reduction of Nitrogen Oxides with Propene in the Presence of Oxygen," *Applied Catalysis B: Environmental*, Vol. 44, No. 4, 2003, pp. 355-370. doi:10.1016/S0926-3373(03)00103-6

[10] Y. Teraoka, K. Torigoshi, H. Yamaguchi, T. Ikeda and S. Kagawa, "Direct Decomposition of Nitric Oxide over Stannate Pyrochlore Oxides: Relationship between Solid-State Chemistry and Catalytic Activity," *Journal of Molecular Catalysis A*: *Chemical*, Vol. 155, No. 1-2, 2000, pp. 73-80. doi:10.1016/S1381-1169(99)00320-9

[11] S. Iwamoto, R. Takahashi and M. Inoue, "Direct Decomposition of Nitric Oxide over Ba Catalysts Supported on CeO_2-Based Mixed Oxides," *Applied Catalysis B*: *Environmental*, Vol. 70, No. 1-4, 2007, pp. 146-150. doi:10.1016/j.apcatb.2006.01.016

[12] H. Iwakuni, Y. Shinmyou, H. Matsumoto and T. Ishihara, "Direct Decomposition of NO into N_2 and O_2 on $SrFe_{0.7}Mg_{0.3}O_3$ Perovskite Oxide," *Bulletin of the Chemical Society of Japan*, Vol. 80, No. 10, 2007, pp. 2039-2046. doi:10.1246/bcsj.80.2039

[13] T. Ishihara, Y. Shinmyou, K. Goto, N. Nishiyama, H. Iwakuni and H. Matsumoto, "NO Decomposition on Ruddlesden-Popper-Type Oxide, $Sr_3Fe_2O_7$, Doped with Ba and Zr," *Chemistry Letters*, Vol. 37, No. 3, 2008, pp. 318-319. doi:10.1246/cl.2008.318

[14] H. Iwakuni, Y. Shinmyou, H. Yano, K. Goto, H. Matsumoto and T. Ishihara, "Effects of Added CO_2 and H_2 on the Direct Decomposition of NO over $BaMnO_3$-Based Perovskite Oxide," *Bulletin of the Chemical Society of Japan*, Vol. 81, No. 9, 2008, pp. 1175-1182. doi:10.1246/bcsj.81.1175

[15] Y. Teraoka, K. Torigoshi and S. Kagawa, "Inhibition of NO Decomposition Activity of Perovskite-Type Oxides by Coexisting Carbon Dioxide," *Bulletin of the Chemical Society of Japan*, Vol. 74, No. 6, 2001, pp. 1161-1162. doi:10.1246/bcsj.74.1161

[16] K. Goto, H. Matsumoto and T. Ishihara, "Direct Decomposition of NO on Ba/Ba-Y-O Catalyst," *Topics in Catalysis*, Vol. 52, No. 13-20, 2009, pp. 1776-1780. doi:10.1007/s11244-009-9337-7

[17] T. Ishihara and K. Goto, "Direct Decomposition of NO over BaO/Y_2O_3 Catalyst," *Catalysis Today*, Vol. 164, No. 1, 2011, pp. 484-488. doi:10.1016/j.cattod.2010.12.005

[18] K. Goto and T. Ishihara, "Direct Decomposition of NO into N_2 and O_2 over $Ba_3Y_{3.4}Sc_{0.6}O_9$," *Applied Catalysis A*: *General*, Vol. 409-410, No. 1, 2011, pp. 66-73. doi:10.1016/j.apcata.2011.09.027

[19] G. Adachi and N. Imanaka, "The Binary Rare Earth Oxides," *Chemical Reviews*, Vol. 98, No. 4, 1998, pp. 1479-1514. doi:10.1021/cr940055h

[20] N. Imanaka, T. Masui and H. Masaki, "Direct Decomposition of Nitric Oxide over C-Type Cubic $(Gd_{1-x-y}Y_xBa_y)_2O_{3-y}$ Solid Solutions," *Advanced Materials*, Vol. 19, No. 21, 2007, pp. 3660-3663. doi:10.1002/adma.200602323

[21] H. Masaki, T. Masui and N. Imanaka, "Direct Decomposition of Nitric Oxide into Nitrogen and Oxygen over C-Type Cubic Y_2O_3-ZrO_2 Solid Solutions," *Journal of Alloys and Compounds*, Vol. 451, No. 1-2, 2008, pp. 406-409. doi:10.1016/j.jallcom.2007.04.158

[22] N. Imanaka and T. Masui, "Advanced Materials for Environmental Catalysts," *The Chemical Record*, Vol. 9, No. 1, 2009, pp. 40-50. doi:10.1002/tcr.20167

[23] S. Tsujimoto, K. Mima, T. Masui and N. Imanaka, "Direct Decomposition of NO on C-Type Cubic Rare Earth Oxides Based on Y_2O_3," *Chemistry Letters*, Vol. 39, No. 5, 2010, pp. 456-457. doi:10.1246/cl.2010.456

[24] S. Tsujimoto, X. Wang, T. Masui and N. Imanaka, "Direct Decomposition of NO into N_2 and O_2 on C-type Cubic Y_2O_3-ZrO_2 and Y_2O_3-ZrO_2-BaO," *Bulletin of the Chemical Society of Japan*, Vol. 84, No. 7, 2011, pp. 807-811. doi:10.1246/bcsj.20100360

[25] S. Tsujimoto, C. Nishimura, T. Masui and N. Imanaka, "Coexisting Gas-Resistant C-type Cubic Yb_2O_3-Tb_4O_7 Catalysts for Direct NO Decomposition," *Chemistry Letters*, Vol. 40, No. 7, 2011, pp. 708-710. doi:10.1246/cl.2011.708

[26] N. Imanaka and T. Masui, "Advances in Direct NO_x De-

composition Catalysts," *Applied Catalysis A*: *General*, Vol. 431-432, No. 1, 2012, pp. 1-8. doi:10.1016/j.apcata.2012.02.047

[27] R. D. Shannon, "Revised Effective Ionic Radii and Systematic Studies of Interatomic Distances in Halides and Chalcogenides," *Acta Crystallographica Section A*, Vol. 32, No. 5, 1976, pp. 751-767. doi:10.1107/S0567739476001551

